Easy and accurate mechano-profiling on micropost arrays

Goedecke, Nils ; Bollhalder, Maja ; Bernet, Remo ; Silvan, Unai ; Snedeker, Jess

Abstract: Cell culture substrates with integrated flexible microposts enable a user to study the mechanical interactions between cells and their immediate surroundings. Particularly, cell-substrate interactions are the main interest. Today micropost arrays are a well-characterized and established method with a broad range of applications that have been published over the last decade. However, there seems to be a reservation among biologists to adapt the technique due to the lengthy and challenging process of micropost manufacture along with the lack of easily approachable software for analyzing images of cells interacting with microposts. The force read-out from microposts is surprisingly easy. A micropost acts like a spring with the cell ideally attached at its tip. Depending on size a cell applies force from its cytoskeleton through one or multiple focal adhesion points to the micropost, thus deflecting the micropost. The amount of deflection correlates directly to the applied force in direction and in magnitude. The number of microposts covered by a cell and the post deflection patterns are characteristic and allow determination of values like force per post and many biologically relevant parameters that allow "mechano-profiling" of cell phenotypes. A convenient method for mechano-profiling is described here combining the first generation of ready-to-use commercially available microposts with an in-house developed software package that is now accessible to all researchers. As a demonstration of typical application, single images of bone cancer cells were taken in bright-field microscopy for mechano-profiling of cell line models of metastasis. This combination of commercial traction force sensors and open source software for analysis allows for the first time a rapid implementation of the micropost array technique into routine lab work done by non-expert users. Furthermore, a robust and streamlined analysis process enables a user to analyze a large number of micropost images in a highly time-efficient manner.

DOI: https://doi.org/10.3791/53350

Video Article

Easy and Accurate Mechano-profiling on Micropost Arrays

Nils Goedecke[1], Maja Bollhalder[1], Remo Bernet[1], Unai Silvan[1], Jess Snedeker[1,2]

[1]University of Zurich, Balgrist University Hospital

[2]Institute for Biomechanics, ETH Zurich

Correspondence to: Jess Snedeker at snedeker@ethz.ch

URL: http://www.jove.com/video/53350
DOI: doi:10.3791/53350

Keywords: Bioengineering, Issue 105, mechanobiology, cell adhesion, cell mechanics, contractility, extracellular matrix, traction force microscopy, mechanosensitive assay

Date Published: 11/17/2015

Citation: Goedecke, N., Bollhalder, M., Bernet, R., Silvan, U., Snedeker, J. Easy and Accurate Mechano-profiling on Micropost Arrays. *J. Vis. Exp.* (105), e53350, doi:10.3791/53350 (2015).

Abstract

Cell culture substrates with integrated flexible microposts enable a user to study the mechanical interactions between cells and their immediate surroundings. Particularly, cell-substrate interactions are the main interest. Today micropost arrays are a well-characterized and established method with a broad range of applications that have been published over the last decade. However, there seems to be a reservation among biologists to adapt the technique due to the lengthy and challenging process of micropost manufacture along with the lack of easily approachable software for analyzing images of cells interacting with microposts.

The force read-out from microposts is surprisingly easy. A micropost acts like a spring with the cell ideally attached at its tip. Depending on size a cell applies force from its cytoskeleton through one or multiple focal adhesion points to the micropost, thus deflecting the micropost. The amount of deflection correlates directly to the applied force in direction and in magnitude. The number of microposts covered by a cell and the post deflection patterns are characteristic and allow determination of values like force per post and many biologically relevant parameters that allow “mechano-profiling” of cell phenotypes.

A convenient method for mechano-profiling is described here combining the first generation of ready-to-use commercially available microposts with an in-house developed software package that is now accessible to all researchers. As a demonstration of typical application, single images of bone cancer cells were taken in bright-field microscopy for mechano-profiling of cell line models of metastasis. This combination of commercial traction force sensors and open source software for analysis allows for the first time a rapid implementation of the micropost array technique into routine lab work done by non-expert users. Furthermore, a robust and streamlined analysis process enables a user to analyze a large number of micropost images in a highly time-efficient manner.

Video Link

The video component of this article can be found at http://www.jove.com/video/53350/

Introduction

Mechano-sensitive cell-based assays allow for investigating adherent cells, with a broad range of applications that reflect the central role that mechanics can play in cell biology. These applications often focus on the underlying mechanisms that drive subcellular processes or whole-cell behavior. On the one hand, external environmental factors such as extra cellular matrix composition or matrix stiffness can dramatically affect the mechanical and biological response of a cell.[1] The same can be observed after use of many classes of pharmaceutically active compounds, the effects of which are often characterized using cell culture models.[2] On the other hand genotypic properties, such as those caused by spontaneous or experimentally induced genetic mutations, can induce marked changes in cell phenotype that are associated with alterations in the cytoskeleton structure and function.[3] These examples are just a few of the many possible topics for which mechanical phenotyping of cells is relevant, and all of these have been usefully investigated with micropost arrays.

At time of this writing, approximately 200 articles have been published describing cell-micropost interaction. These works discuss theoretical aspects of micropost deflection principles as well as practical instructions on their manufacture. The first article describing the interaction of cells and flexible micropost arrays was published by Tan and colleagues in 2003.[4] In contrast to classic traction force microscopy (TFM) where continuous soft substrates are used to estimate nanonewton-scale cell contractility, Tan *et al*. described a method using multiple closely spaced vertical beams made of silicone elastomer. The main advantages of this technique emerge from two major features. First in order to change the cell-apparent substrate stiffness one only needs to change the micropost dimensions while keeping the substrate composition otherwise constant and thus avoiding differences in surface topology and chemistry. Second microposts act like individual springs that can be discretely analyzed with force and spatial resolutions on the order of individual focal adhesions and can reduce the analytical challenges that are inherent to analogous analysis by standard TFM.

Today the range of applications for micropost arrays greatly exceeds just the mapping of forces for a few single cells. For example, Akiyama reports the use of an isolated dorsal vessel tissue from a moth caterpillar as an actuator for a micropost array, in order to develop an insect muscle-powered autonomous micro-robot.[5]

However, most published applications of microposts have focused on studies of medical conditions like infection or cancer. For instance, micropost arrays have been used to study the force generation of bundled type IV pili of Neisseria gonorrhoea colonies that is associated with signal cascades enhancing infection.[6] Others have used microposts to study breast cancer cells treated with pharmaceutical compounds targeting the cytoskeleton.[7]

Deflection of a micropost is often described using classical beam theory for a cantilever with an end load assuming the cell attaches only to the very tip of the micropost. Here the applied force *F* that causes a deflection *δ* depends on the micropost's "bending stiffness" *k* and is calculated by:

$$F = k\,\delta = \left(\frac{3\,E\,I}{L^3}\right)\delta \quad (1)$$

with E, I, and L being the Young's modulus, area moment of inertia and beam length respectively. However, results from this equation only give a general approximation of the forces at work since beam shearing and bending as well as substrate warping are not taken into account. Considering that microposts are typically made from soft materials like polydimethylsiloxane (PDMS)-based silicone rubber these factors need to be included. Schoen *et al.* demonstrated that there is such a correction factor based on the aspect ratio of the micropost (L/D) and the corresponding polymer's Poisson ratio *v*.[8] It is given by:

$$corr = \frac{\frac{16}{3}\left(\frac{L}{D}\right)^3}{\frac{16}{3}\left(\frac{L}{D}\right)^3 + \frac{7+6v}{3}\frac{L}{D} + 8\,T_{tilt}(v)\left(\frac{L}{D}\right)^2} \quad (2)$$

With $T_{tilt}(v)$ being a tilting coefficient that includes fitting parameter a = 1.3 as can be found in the same article:

$$T_{tilt}(v) = a\,\frac{1+v}{2\pi}\left\{2(1-v) + \left(1 - \frac{1}{4(1-v)}\right)\right\} \quad (3)$$

That means a micropost's corrected stiffness k_{corr} is the product of the pure bending stiffness k=k_{bend} and the correction factor *corr* given by:

$$k_{corr} = k_{bend} \cdot corr\ with\ corr = \frac{\delta_{bend}}{\delta_{bend} + \delta_{shear} + \delta_{tilt}} \quad (4)$$

Therefore, cell force calculations should be performed using the more refined variation of equation (1) now reading:

$$F = k_{corr}\,\delta \quad (5)$$

The impact of the correction becomes more obvious as soon as typical values for micropost dimensions are used. For example, a 15-micron long micropost with a circular cross section and a diameter of 5 µm made of PDMS-based silicone rubber leads to a correction factor of 0.77 and therefore an uncorrected calculation would overestimate the exerted cell forces by 23%. This becomes even more severe for microposts with smaller aspect ratios.

Traditionally, micropost image analysis has also been based on idealized beam bending theory. In 2005 the group that pioneered the use of micropost arrays published an image analysis software suited for micropost analysis.[9] The software requires a software license and the user must take three images for each position; one each from the micropost's top and bottom planes in transmission mode and another one in fluorescence mode with the stained cell. After comparing the top and bottom positions for each micropost the software determines a force vector field and calculates related parameters like force per post. Other software packages exist and their analysis principles are briefly mentioned in the corresponding articles that describe them, but these analytical software packages are generally not publicly available.[10,11]

The micropost arrays designed for mapping cell forces can be classified as either being in an orthogonal micropost layout or a hexagonal one, the latter of which have the advantage of equidistant gaps between all neighbor microposts. Typical microposts have a circular cross section and their dimensions range from 1.0 µm to 10 µm in diameter and 2 to 50 µm in length. [4] However, microposts with elliptic or square cross section have also been reported.[12,13]

The use of PDMS-based silicone mixtures as micropost material allows for adding nanoparticles into the mixture. For example adding cobalt nano-rods enables a magnetic activation of the micropost and thus gives another degree of freedom to potential experimental designs.[14] Most groups produce their micropost arrays on flat rigid substrates like cover glass or inside a Petri dish. However, Mann and co-workers recently reported a micropost array formed on a stretchable membrane.[15] This allows the application of cell stretching forces to adherent cells while studying live-cell subcellular dynamic responses in terms of cell contractility.

The widely employed and most established process for making micropost arrays is based on soft lithography as described in the insightful protocols of Sniadecki and colleagues.[16-18] In short standard cleanroom processes are used to generate the microstructures on top of a silicon wafer using SU8 photoresist. This is followed by a copying process wherein the silicone rubber is cast over the structures transferring them into molds. In a second step these molds are used to replicate the initial microstructure using silicone rubber on top of a chosen substrate. However despite the large and growing number of publications related to their application, establishing a manufacturing process for microposts takes

considerable amount of time even for micro-engineering experts; there are many process steps that require optimization and adaptation to the specific lab environment and micropost layout to yield an acceptable quality level.

Commercial micropost arrays are now available in a ready-to-use ("off-the-shelf") format with a consistently high quality. As such they are an alternative to the complex and lengthy manufacturing process required for on-site production. In this paper a commercially available micropost array was used for mapping cellular forces using a single bright-field microscopy image. More importantly this article describes and documents a fully-functional open-source software named MechProfiler, which is available for download as supplementary material to this manuscript. An actively maintained version of the software can also be found at http://www.orthobiomech.ethz.ch.

The combination of an "off-the-shelf" assay and a compatible open-source analysis software markedly lowers the entry hurdle to achieve accurate TFM experiments. Researchers without access to either clean room facilities or software development expertise can analyze cellular forces successfully. It enables a user to focus on the mechanosensitivity assay output rather than the technology itself, and makes traction force measurements available to a broader community. Furthermore, this is an important step to pave the way towards fully automatic screening of micropost arrays.

The MechProfiler analysis software processes images in file format tiff, png, bmp and jpg. The images can be taken using fluorescence, phase contrast or bright-field light microscopy. The standalone program runs together with the free Matlab Compiler Runtime (available at: **Figure 12**) and underlying algorithms allow for streamlined image processing, which enables the user to process images with single or multiple cells in about 1 min. Further, these cells may either be living or "fixed".

The MechProfiler software is able to greatly increase data analysis throughput by relying on reproducibility of quality commercial micropost arrays, more specifically, the default "non-deflected" position of each post in the array can be presumed against an ideal grid (manufacturing deviations for the grid in the arrays used for this study were less than 100 nm).

In short one opens a selection of image files for analysis, crops them to the region of interest, defines the posts covered by cells or which need to be discarded, determines the post positions, calculates the deflections/forces against the ideal grid, and finally saves all cell-specific data with a possibility for export, including to a standard office spreadsheet.

Protocol

1. Culturing Cells on Micropost Arrays

Note: All steps must be performed in a biosafety cabinet to ensure sterility. The volumes given here are for T25 cell culture flasks. The cell culture medium recipe and cell seeding density are optimized for bone cancer cell lines HuO9 and M132.

1. Prepare a cell culture for seeding onto a micropost array.
    1. Inspect the cell culture quality by placing the culture flask on a standard light microscope. Ensure that the cells show a typical growth and morphology by estimating how much of the culture flask bottom is covered. A coverage of 70%-80% reflects a healthy growth rate. Pay attention to the amount of floating cells as they represent dead cells and/or an overgrown culture.
    2. Trypsinize cells by removing medium and washing with 4 ml 1x Phosphate buffered saline (PBS) buffer. Add 0.8 ml 1x Trypsin/ Ethylenediaminetetraacetic acid (EDTA) and incubate at RT until the cells dislodge, which takes about 2-4 min. Check the process with the microscope and occasionally tap the flask gently to support the dislodging.
    3. Add 5 ml cell culture medium (Dulbecco's modified Eagle medium (DMEM)/F12 with 10% fetal bovine serum (FBS), 1% penicillin/ streptavidin (Pen/Strep)) to stop the reaction and to wash off residual cells that still sit on the flask's bottom. Subsequently pipette this suspension up and down several times to gain a homogenous mixture. Make sure to pipette all solutions across the original growth area of the flask to gain an effective dislodging.
    4. Transfer the cell suspension in to a 15 ml tube and centrifuge it using a table top centrifuge at 0.5 x g for 3 min.
    5. Remove the supernatant and re-suspend the cell pellet in 5 ml medium by pipetting up and down 5 times. Make sure to avoid the generation of bubbles while doing so.
    6. Determine cell density by using a cell counting chamber and a light microscope. Check the cell suspension in cell counting chamber for cell aggregates and ensure to have only single cells for the subsequent experiment. Pipette again up and down several times if the cells tend to form aggregates to separate them.
    7. Dilute the cell suspension with sufficient medium to gain a cell solution of 25,000 cells/ml. Mix it well by inverting the closed tube several times.

2. Prepare a micropost array for cell seeding.
   Critical Note: Do not pipette onto the micropost array directly as this could potentially harm the microposts, especially when unwanted bubbles are introduced. Furthermore, make sure that the micropost array never dries out as occurring capillary forces lead to collapsing of the microposts.
    1. Place the glass substrate with the micropost array face up in a well of a 12-well plate by using a pair of tweezers and wet it by adding 1 ml ethanol (99%). Incubate at RT for 20-30 sec.
    2. Dilute the ethanol stepwise by adding approximately 1 ml sterile de-ionized water (DI water) on the well side and aspirating roughly 1 ml using a transfer pipette or aspiration device. Repeat this step at least 3 times.
    3. Replace the DI-water with PBS-buffer in the same manner by adding and aspirating approximately 1 ml. Repeat this step 3 times.
    4. Replace the PBS-buffer with medium by adding and aspirating approximately 1 ml of medium. Repeat this step 3 times.

3. Pipette 1 ml cell solution (25,000 cells) on top of each prepared micropost array. Close multi-well plate and transfer it to an incubator (CO_2 5%, 37 °C). Let the cells adhere and grow on top of microposts for 6 -7 hr.

4. Inspect the adhesion process occasionally by using a light a microscope. Check that most of the cells appear spread out across multiple microposts.

2. Fixing & Staining Cells

Note: All steps and volumes given here are for a single well of a 12-well plate. It is recommended to process not more than four of the twelve wells at a time to avoid a drying out of the wells after aspiration of any liquid, which will result in a collapse of the microposts.

1. Aspirate medium from the well and wash cells 2x with 1 ml PBS-buffer. Make sure to apply a gentle force while washing with PBS to remove cell debris that accumulated on the micropost array during incubation and to detach dead cells.
2. Fix the cells with 0.5 ml 3.7% buffered formaldehyde solution for 5 min.
3. Replace the formaldehyde solution by washing the micropost array 2x with 1 ml sterile DI water.
4. Stain the cells with dye (0.05% Coomassie Brilliant Blue in 50% water, 40% ethanol and 10% acetic acid) for about 90 sec. Wash excess staining solution off 2x with 1 ml sterile DI water. Add 1 ml DI water to micropost array.
5. Check staining result using a light microscope. Repeat the staining step, if cell body is too faint to be visualized.
6. Store micropost arrays with the stained cells on top in a refrigerator at 4 °C. Ensure to keep them under water at all times.

3. Cell Imaging

Note: Step 4 only applies to microscopes without infinity corrected optics.

1. Add 2 ml DI-water to a Petri dish with a thin glass bottom for high resolution imaging.
2. Transfer micropost array using a pair of tweezers into the imaging dish with the microposts facing up.
3. Place the imaging Petri dish on a moveable stage of a light microscope.
4. Turn the compensation ring of the lens used for imaging until the number on the scale represents the total thickness of all materials along the optical path to compensate for the mismatch in refractive indices of the glass substrate, the silicone elastomer and the liquid on top. This should lead to a bright appearance of the microposts cores.
5. Close the iris on the illumination side down to 50% and remove any phase contrast rings from the optical path enabling an ordinary bright-field mode.
6. Align the micropost array that the microposts form a horizontal line across the observation field. Define a start point (*e.g.,* top left) and move the Petri dish stepwise across the stage scanning the micropost array while taking numerous images.
7. Take all images with the highest resolution setting for the camera using a 20X or 40X objective. Aim to have a single cell in the center of the image.
8. Sweep along the z-axis through the substrate until the micropost tips are in focus. Use the fine tuning focus wheel of the microscope and turn it towards focusing on the micropost bottom for about 2-3 µm.
9. Establish a standard imaging procedure by taking series of test images of one array section sweeping through the imaging parameters one at a time (*e.g.,* exposure time, iris setting, lamp settings *etc.*). Analyze images with MechProfiler and determine a suitable parameter set for a fast and reliable analysis.

4. Image Analysis with Open Source Software “MechProfiler”

Note: All software functions can be activated with a pointing device using the left mouse button. However, a trained operator will use the documented shortcut keys designed to be on the left half of the keyboard to enable an efficient two-handed image processing.

1. Start image analysis software MechProfiler and open a range of images that need to be analyzed by clicking “Open”.
2. Insert all parameters into the “Settings” section given by the software developer. Determine the parameters that must be custom configured (*i.e.,* contour threshold and minimal distance) according to the procedures described in detail by the software manual.
3. Analyze images one-by-one by cropping them to the area of interest by using “Crop” (click and drag with the mouse button pressed down). Double click inside the drawn rectangle to finish this action.
4. Marking each visible cell outline one-by-one by clicking on “Draw cell outlines” and use the cross hair cursor for drawing including all microposts the cell is attached to.
5. Discard any unwanted microposts by clicking “Discard Posts” and use the cross hair cursor for drawing. Enclose all microposts that belong to a cell outside of the image section or that are deflected for any other reason but not by the cell of interest.
6. Start the software subroutine “Find Centroids” by mouse click. Adjust the filter setting right next to the “Find Centroids” button until all microposts are registered, which is visible by a red cross in their center. If the filter setting is too low microposts will be ignored, if it is too high multiple positions will be marked for a single micropost. Keep the filter setting constant during an analysis session.
7. Use the manual editing function “Manual Edit” for centroids with multiple or missed micropost positions. Use the mouse cross hair to select the micropost in question by clicking and dragging it across. Double click inside the rectangle and place the missing red marker in the enlarged image section, which automatically closes. Discard such a micropost if it is outside the drawn cell outline (see step 4.5) before proceeding.
8. Find the ideal micropost grid by activating the “Generate Grid” function with a mouse click. Ensure the position corresponds with the true micropost head, shown by a blue ring, inside the drawn cell outline.
9. Correct any misplaced grid maker inside the cell area where needed using the corresponding “Manuel Edit” function with a mouse click. Use the cross hair to select the micropost in question by clicking and dragging it across. Double click inside the appearing rectangle and place the missing blue marker in the enlarged image section, which automatically closes.
10. Use the button “Calculate Deflections” by mouse click to get a histogram of the calculated deflection values based on the difference between a micropost’s position inside the image section and the generated ideal grid.
11. Save the complete analysis including the tables of values by a mouse click on “Save”.

12. Continue the image analysis either by clicking on “Reset View” and analyze another image section or mouse click on “Next Image”, which conveniently can be done using the right keyboard curser key.

5. Data Analysis — Mechanoprofiling

1. Open the file “results.xls” with an office spreadsheet program from the folder with the analyzed images. It contains the data with all calculated values including all micropost deflections and standard derivative measures such as work (*i.e.,* substrate deformation energy) by the analyzed cell.

Representative Results

The main advantage of the described technique lies in its simplicity and potential for rapid and effective integration into routine lab work. The combination of high quality commercial sensor arrays paired with open-source software provides information about mechano-sensitivity that would otherwise requires access to cleanroom facilities and in-depth knowledge of image analysis and software development. **Figure 1** illustrates the workflow of the presented method. It starts with preparing and seeding cells onto the micropost array. After fixing and staining the cells the micropost arrays are ready for imaging. The central part of the technique is the image analysis using the MechProfiler software. A user can start analyszng images immediately after entering all relevant parameters in the “Settings” of the GUI. The corresponding pixel size is the length that is represented by a single pixel and depends on the user’s setup. It needs to be established separately for each used magnification by taking images of objects with known size. An example is given in the supplementary **Figure 9**.

Image quality is a key factor as it strongly influences the analysis process. In order to achieve the highest quality one should make sure to have a stable and routinely serviced imaging platform as shown in **Figure 2.** In particular, the alignment of the light source is important as misalignment will cause unwanted shadows that can be problematic when analyzing the images. Furthermore, placing the light microscope atop an anti-vibration table or plate is beneficial in most laboratories as it gives additional stability during imaging.

The advantages of using a thin glass bottom Petri dish for imaging include higher effective numerical aperture values that translates to brighter images with increased resolution.

When taking the images in bright-field mode a 50% closed iris is recommended, as focusing on the microposts tips is facilitated due to the circumferences appearing as a crisp dark ring. Moreover, in case the used objective has a compensation ring, it is essential to set it correctly to achieve accurate force readouts. The impact of that feature can be seen by comparing **Figure 3A** and **Figure 3B.** Images that can be quickly analyzed are achieved by combining the correct setting of the compensation ring together with optimal illumination as shown in **Figure 3C**. Strong contrast between a micropost and its surrounding reduces the analysis time as it speeds the searching algorithm. Users will find that only minimal experience is required to achieve images that can be analyzed with ease.

Importantly, the protocols above overcome a critical and common obstacle to rapid and effective integration of micropost arrays into routine lab work. This obstacle stems from the need to control array quality — a demand that is achievable only by thorough and detailed experimental characterization of sensor reproducibility, sensitivity, and accuracy. However, by turning to commercially available micropost arrays this sizeable hurdle is completely avoided. **Figures 4A** and **4B** illustrate the accuracy of such a micropost array. The deviation of the microposts position is well under 200 nm and as such comparable with a “pixel error” that accompanies the camera/objective combination that resulted in a pixel size of 82 nm for the used setup. The analysis of images with cells deflecting the microposts demonstrates that the values for a cell-imposed deflection are substantially higher than 200 nm (as shown in **Figure 4C** and **Figure 4D**) leading to a comfortable signal to noise ratio.

Figure 5 illustrates the different kinds of appearances for microposts within an image depending whether it is deflected or not. As mentioned above non-deflected microposts have a bright circular appearance with a dark ring around them. Their position can be determined using a Hough transformation, which is a feature extraction technique for digital image analysis.

Furthermore, it shows that deflected microposts on an inverted microscope show two facing dark half-moon shapes (see **Figure 5A**). In an upright microscope the edge of the micropost tip and one dark half-moon shape are properly visible whereas the second one becomes difficult to detect. These characteristics are the basis for calculating the positions of bright field microscope images of the tips from deflected microposts, which has been developed for this protocol and was named “Contour Approach”.

Figure 5B is one example of a HuO9 bone cancer cell on microposts imaged on an inverted microscope (top). The analyzed version of that image shows the results from the applied contour approach (bottom). **Figure 5C** was taken using the same micropost array with an upright microscope (top). Again the analyzed version shows the results from using the contour approach.

Every image analysis session starts by a user verification of the parameters in the “Settings” section of the MechProfiler. Some are given by the micropost manufacturer like micropost array dimensions and spring constant. Others are defined by the user such as the values for the contour threshold and a minimal deflection threshold according to procedures detailed in the software manual. However, it is important to note that these values should be chosen carefully and must be constant for all images within an interrelated set of images to guarantee comparability. Whereas the pre-processing steps for the image analysis, like cropping, are self-explaining the underlying strategies for the software functions like “Finding Centroids**”,** “Generate Grid” and the “Contour Approach” need more detailed explanations.

Algorithmic detection of default micropost position (as delivered by the manufacturer) begins by using the “Finding centroids” software function. The algorithm starts in the top left corner of an image searching for the first micropost. Subsequently all other microposts are found based on the coordinates of that first micropost plus the values for the grid and micropost size given by the manufacturer following the hexagonal geometry. The centroid for each found micropost is calculated using a Hough transformation. The filter slider next to the command button of the GUI allows adjusting the sensitivity of this transformation. All found microposts are marked with a red cross and their positions noted for subsequent processes.

Next, the “Generate Grid” function leads to the coordinates of all microposts tips. They are the results from a multi-step process. First an optimization function is solved including the initial positions from the prior executed “Find centroids” algorithm to establish the ideal grid. Second the positions of the microposts inside the cell area are calculated. Microposts with less deflection than defined in the setting parameter “Minimum deflection threshold” relative to the ideal grid are processed with a Hugh transformation. All other micropost tip positions are calculated using the above described contour approach for deflected microposts. Here the software starts searching from the initial centroid away from the cell center for a circular edge (bright to dark) within an angle of 15° (see **Figure 5A**). Once that edge is found a circle with the given micropost diameter is fitted to that edge using the contour threshold value from the settings in the GUI. That parameter determines which pixel grey value is used for the fitting process. The higher that value is the more the fitting leans towards the brighter micropost center the lower that value the more it fits that circle to the darker micropost outline. Once chosen that value should remain constant for all image analyses within a given study to avoid adding artificial deflection or calling deflections too conservatively.

For example, **Figure 6** illustrates the importance of deciding for an appropriate contour threshold value. The software allows the user to choose for a wide range (0.1 to 0.9) to encompass all physically possible illumination situations. The translation of the optical information into deflection distances given for both extremes and a more practical value in the middle are given in **Figure 6B**. However, trained software users often converge to very similar contour threshold values, leading to comparable results as can be seen in **Figure 6C**. Furthermore, using standardized procedures for cell staining and imaging minimizes the risk of invalid contour threshold values, which generally should stay constant within for interrelated sets of images.

In order to demonstrate the robustness of the method a selection of mechano-profiling results are summarized in **Figure 7**. In **Figure 7A** two results from bone cancer cells HuO9 and two from M132 are compared. All four arrays are from the same production batch and therefore have identical mechanical properties. The analysis was performed with a fixed set of parameters for minimal deflection (0.25 µm) and for the contour threshold (0.125). In addition, two identical sets of images from SaOS 2 bone cancer were given to two analysts without further information about parameter settings (see **Figure 7B**). The influence of the staining on the analysis was tested by taking images of bone cancer cells stained with Coomassie Blue R. Subsequently the dye was removed. After re-staining with Coomassie Blue G a second set of images was taken. **Figure 7C** illustrates the results from both series, which were analyzed by the same user with identical values for the minimal deflection (0.25 µm) and the contour threshold (0.25).

A typical example of applied mechano-profiling is presented in **Figure 8A**, wherein the compiled data is presented for the bone cancer cell lines HuO9 and M132 after analyzing 151 cells pooled from each of four arrays. In this overview all indicator values are higher for HuO9 than for M132 already indicating that HuO9 cells apply more force than M132. However, the data from the image analysis contains a large amount of additional single-cell information that can be mined to better understand phenotypic cell line behavior and cell-to-cell variability within a given line. By presenting the results for the force per micropost in a box plot one finds that despite similar minima and maxima, data values are differently distributed and indeed the low metastatic cell line HuO9 cells tend to apply more force than the highly metastatic M132 line (see **Figure 8B**). Furthermore, by categorizing the force values with respect to the cell area one finds that the average force per cell is not only elevated for HuO9 cells compared to M132 but also that the average force per micropost increases as the cells spread until average force per post reaches a more stable value (as can be seen in **Figure 8C**). Moreover for cells covering seven microposts the values are almost identical, which is probably due to the fact that they typically appear in hexagonal shape with one central non-deflected micropost independent of their cell line. Apart from the differences in contractility, morphological differences can be quantified with interesting result. For instance in contrast to the highly metastatic M132 cells there were very few HuO9 cells that covered only three microposts. Other morphological comparisons between the cell lines can be made, including the distribution of cell area represented by the number of microposts covered. **Figure 8D** illustrates that the two cell lines also differ in dynamic spreading behavior when growing on top of microposts. In short, the mechanoprofile for the parental cell line HuO9 reveals that they typically cover more area and apply slightly more force to microposts whereas the metastatic cell line M132, an aggressive cell that derives from HuO9, characteristically covers fewer microposts and applies less force per micropost. These results demonstrate the potential of a TFM based approach for discriminatory applications.

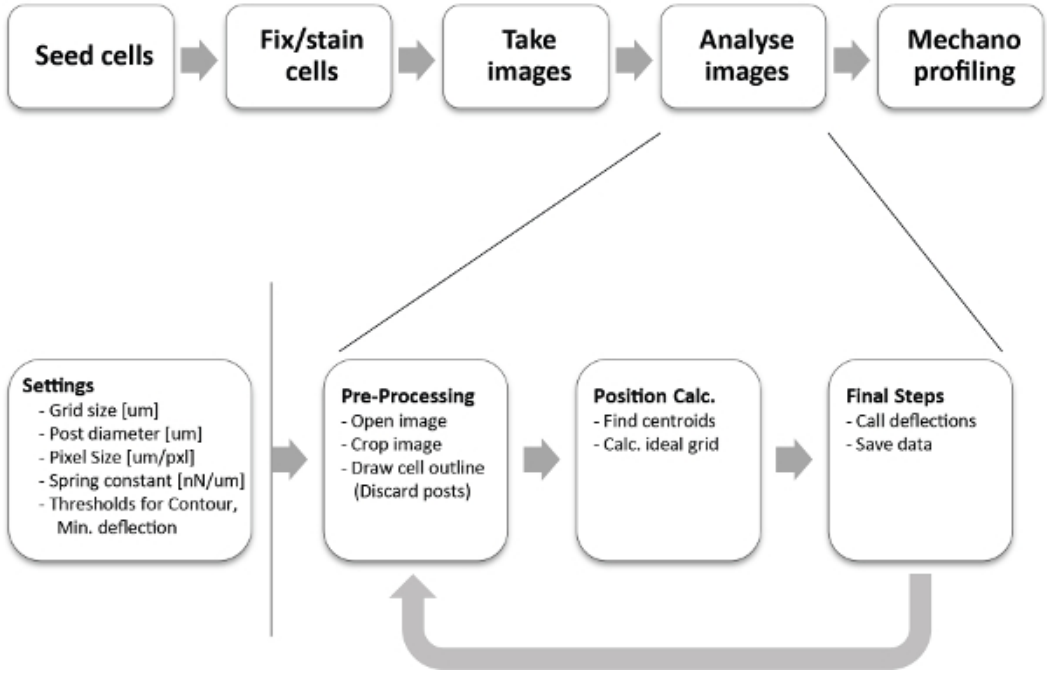

Figure 1. Experiment Workflow. (**A**) The overall procedure contains five consecutive major steps from seeding cells on a micropost array to profiling their mechanical properties. (**B**) The image analysis is performed with the described MechProfiler software. Please click here to view a larger version of this figure.

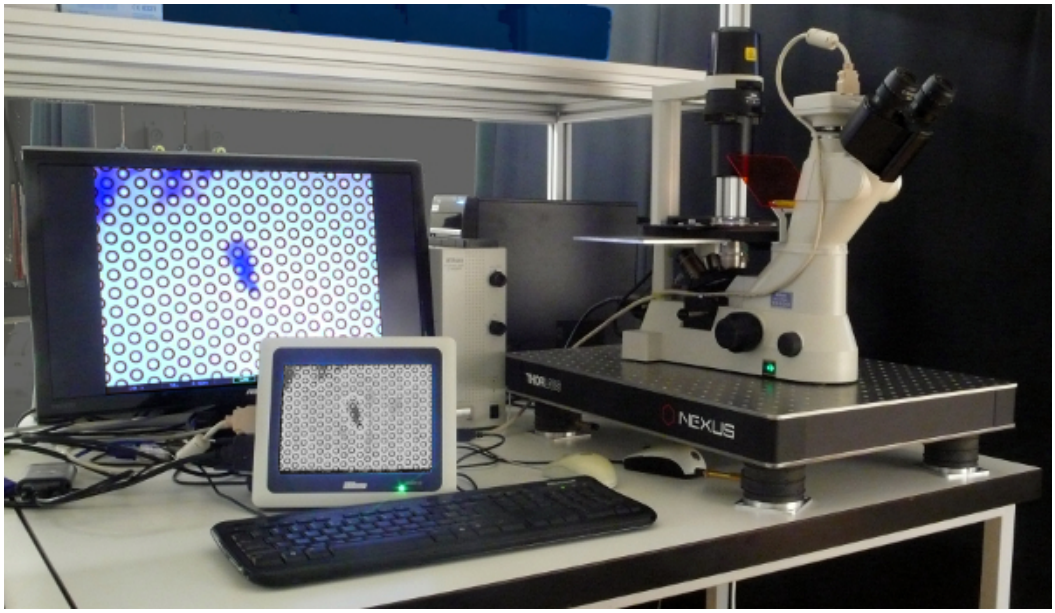

Figure 2. Imaging Setup. A standard inverted microscope is used for imaging the cells on the micropost arrays. The setup also contains a microscope camera and its controller, which can also provide data storage functions. The large screen shown is not essential but nonetheless is convenient for extended imaging sessions. Please click here to view a larger version of this figure.

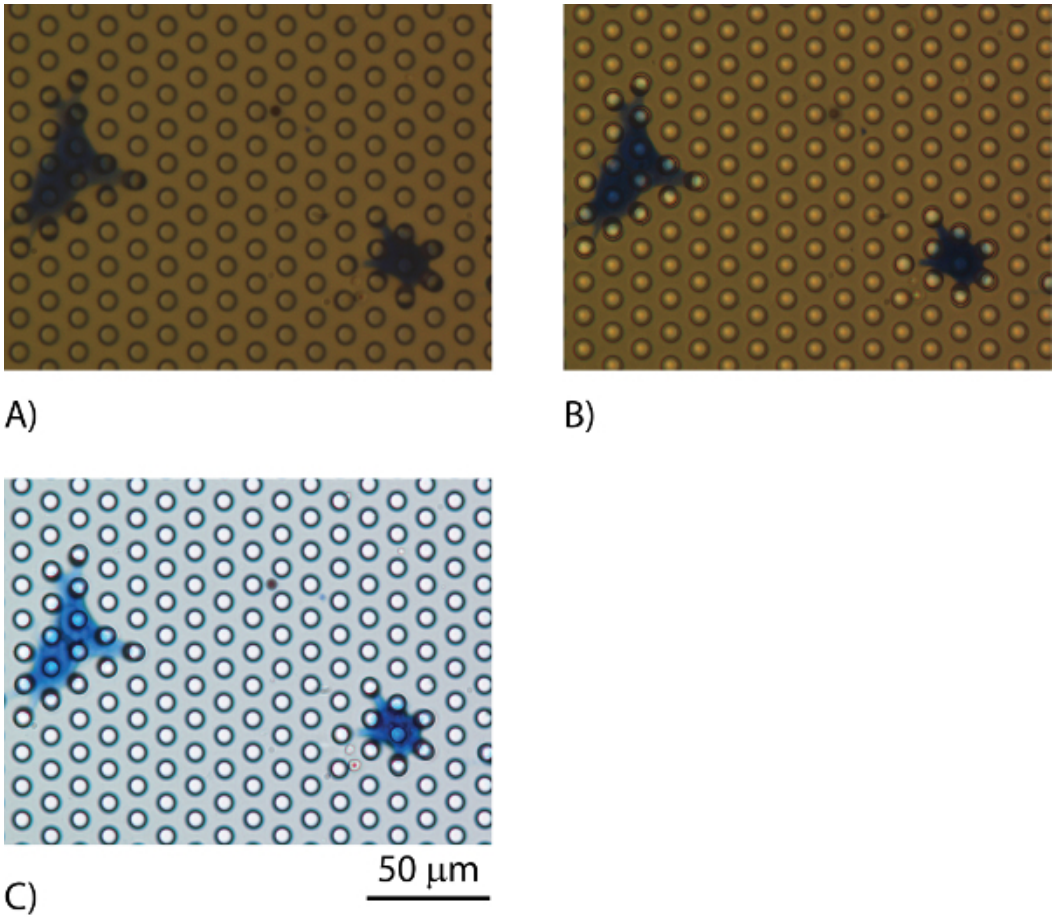

Figure 3. Guideline for micropost imaging. (**A**) Image of stained cells on a micropost array taken with a 40X lens in bright-field mode. Non-deflected microposts appear as dark rings when imaged. Deflected posts assume an elliptic shape with both darker and brighter sub regions. Stained cells that cover microposts makes them appear even darker to the point that there is no contrast between micropost and cell. (**B**) Identical images taken after adjusting the lens compensation ring and re-focusing. Here the cores of the microposts become substantially brighter and give more contrast. (**C**) The same position imaged again after adjusting all illumination parameters with the camera controller. The freely standing microposts appear as bright circles with a dark ring. Deflected microposts show a distinct half-moon “shadow” around the bight core along the pulling axis. Please click here to view a larger version of this figure.>

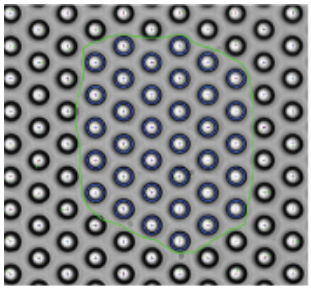

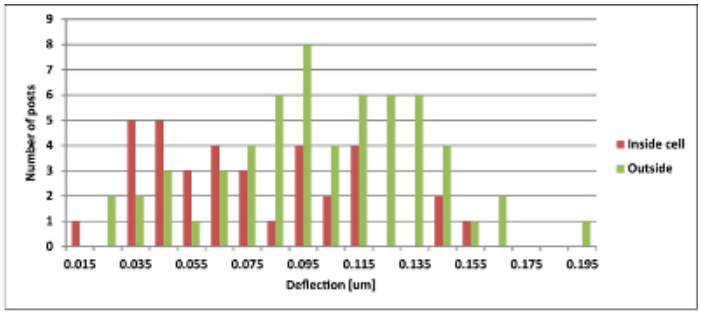

A)

B)

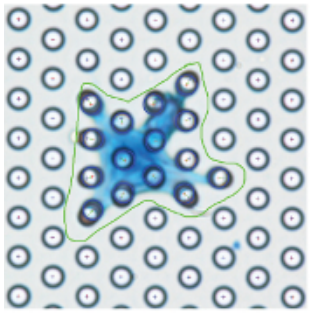

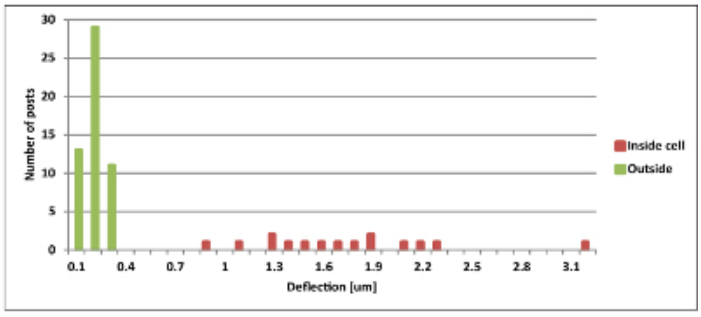

C)

D)

Figure 4. MechProfiler screenshots of analyzed microposts. (**A**) A typical example of an empty micropost array can be seen in this screenshot. The microposts are arranged in a constant hexagonal pattern. (**B**) The histogram with the deflection values for these microposts shows that all values are below 200 nm. (**C**) Typical example for a HuO9 bone cancer cell covering and pulling on multiple microposts. It can be seen that the amount of pulling is heterogeneous. (**D**) The histogram with the deflection values for the HuO9 cell shows the broad spectrum of deflections that arises from the cells' interaction with the micropost substrate. Please click here to view a larger version of this figure.

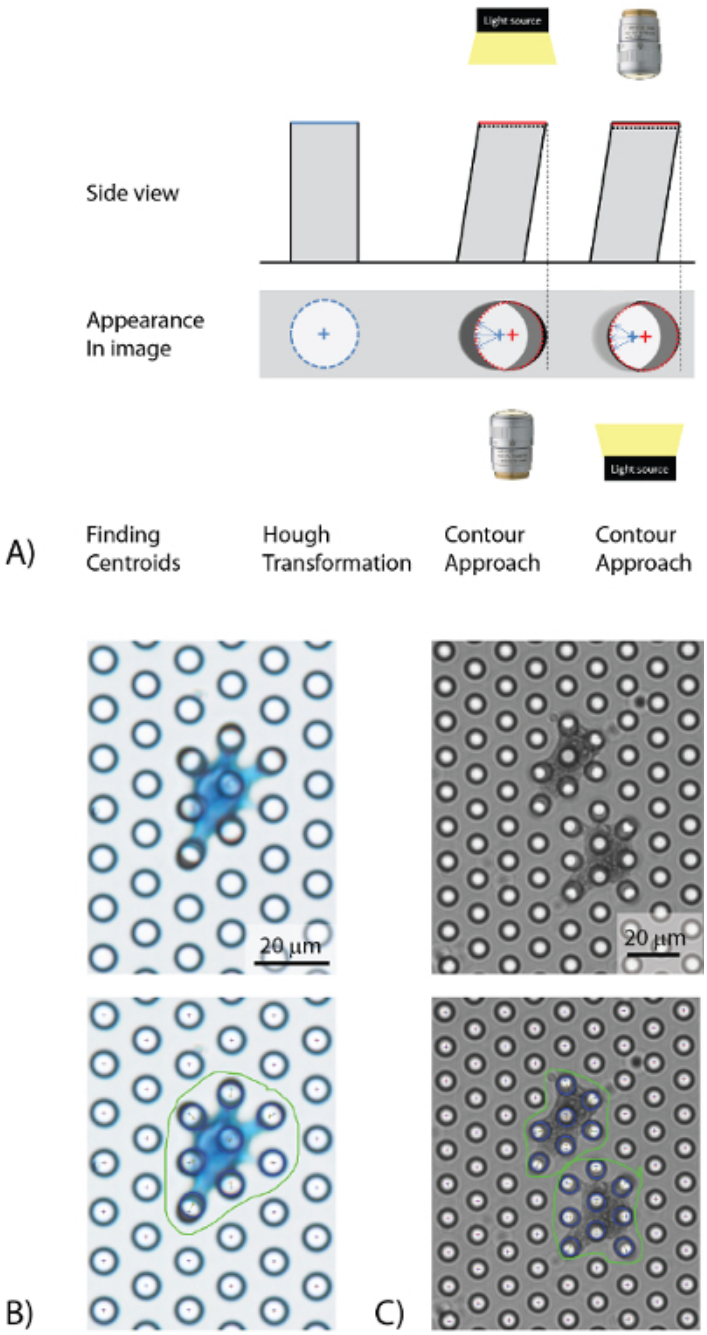

Figure 5. Micropost appearances in bright-field illumination and the strategies for calculating their position within an image. (**A**) Non-deflected microposts appears as a bright circular area with a dark outer ring. The centroid is calculated by a Hough transformation. Deflected microposts show dark half-moon shapes. Depending on the microscope setup if the microposts face the light source (*e.g.,* inverted microscope) there are two well visible half-moon shapes. If the microposts face the lens (*e.g.,* upright microscope) only one half moon is well visible but also the very edge of the tip. In both cases the contour approach should be used to calculate the micropost tip. (**B**) An original image (top) using an inverted microscope from a HuO9 bone cancer cell and its analyzed version (bottom) using the contour approach. (**C**) Original image from the same micropost array (top) using an upright microscope and the analyzed version, again applying the contour approach (bottom) but with a much lower contour threshold value more suitable for calling the dark ring-shaped edge. Please click here to view a larger version of this figure.

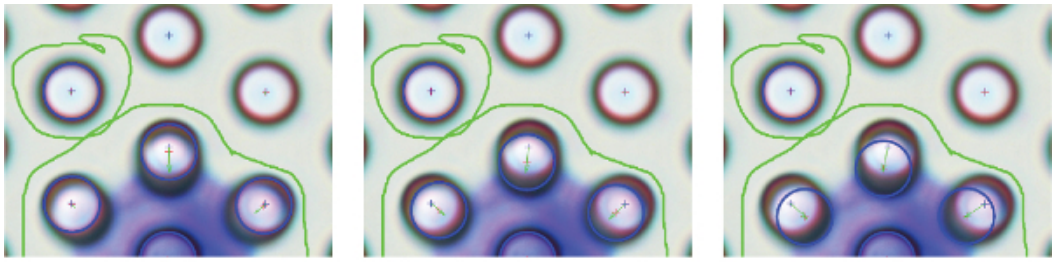

A)

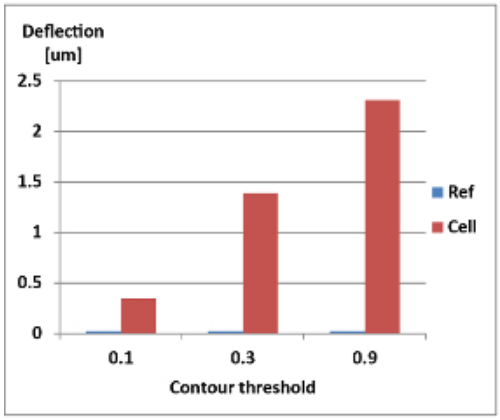

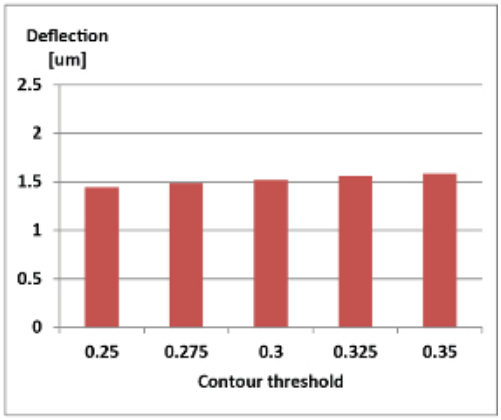

B) C)

Figure 6. The contour approach and choosing the appropriate threshold value. (**A**) The three screenshots illustrate the same analyzed microposts using three different contour threshold values. If the value is set either too low (left) or too high (right) than the software fits the blue ring that represents the micropost head incorrectly. It underestimates or overshoots the real position of the micropost head. A correctly chosen threshold value enables the software to fit that blue ring to the half-moon shaped dark area inside the micropost that forms through deflection. (**B**) The graph shows the average amount of deflection dependent on the chosen contour threshold for the microposts shown in above. It also illustrates that the values for the microposts outside the cell outline are not affected since the contour fitting is not applied there. (**C**) The graph illustrates that choosing a threshold value within a moderate interval minimalizes the risk of over- or underestimating the micropost deflections. The difference between the values chosen by different trained users is normally less than 0.05, which results in acceptable differences in average deflection values. Please click here to view a larger version of this figure.

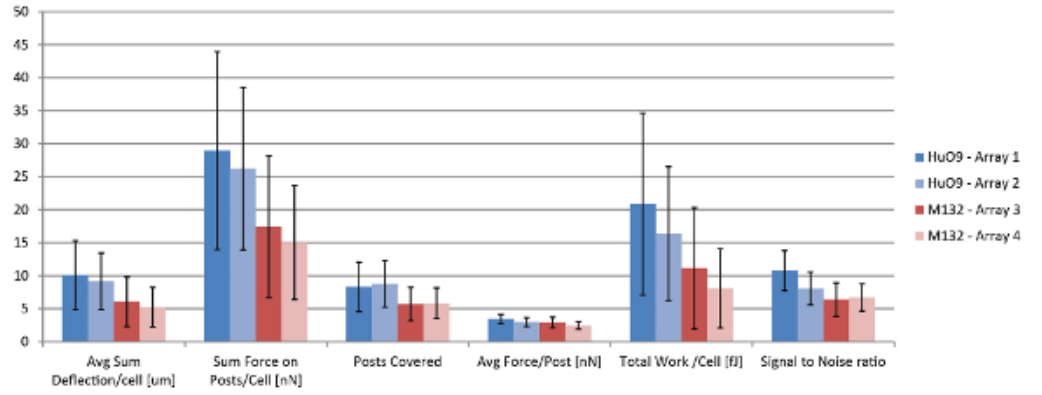

A)

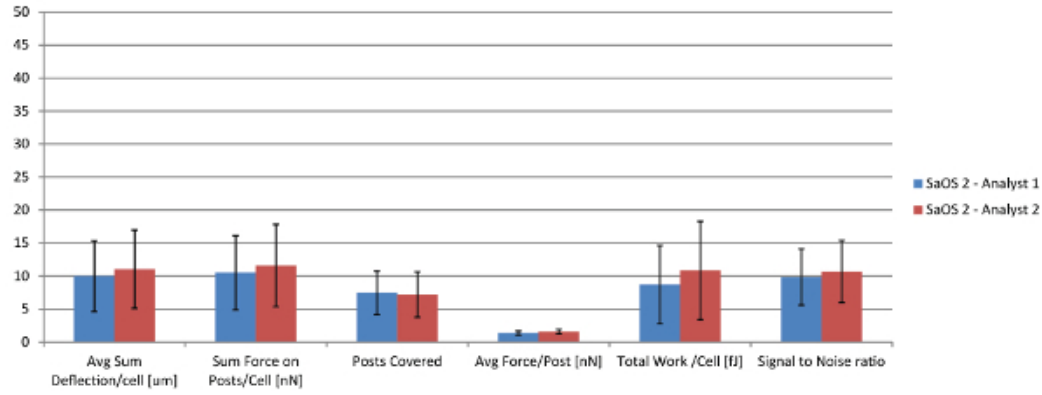

B)

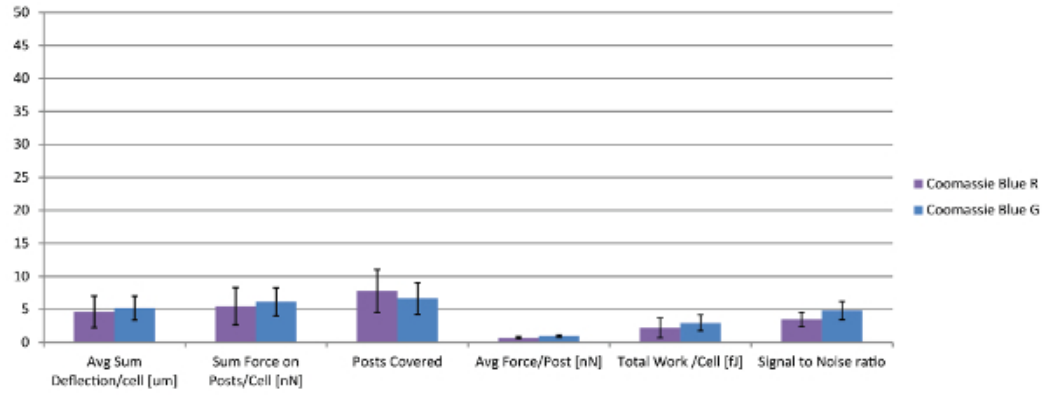

C)

Figure 7. Robustness test for mechano-profile results from different bone cancer cell lines; the error bars represent one standard deviation. (**A**) Mechano-profiling results from four identical micropost arrays after seeding HuO9 cells on array 1 and M132 on array 3 — four days later seeding HuO9 on array 2 and M132 on array 4. (**B**) Comparison of results from mechano-profiling based on identical sets of images after analysis by two independent analysts. (**C**) Comparison of image analysis results from two different image series first one taken after staining with Coomassie Blue R and the second after complete removal of dye and re-staining with Coomassie Blue G. Please click here to view a larger version of this figure.>

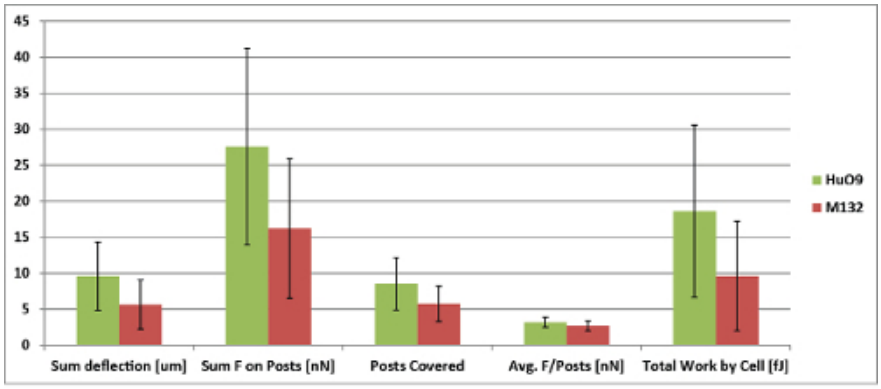

A)

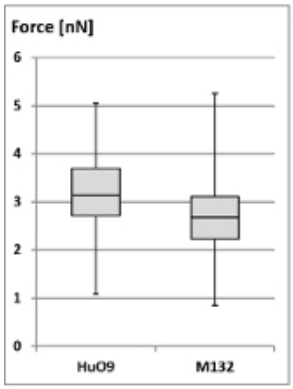

B)

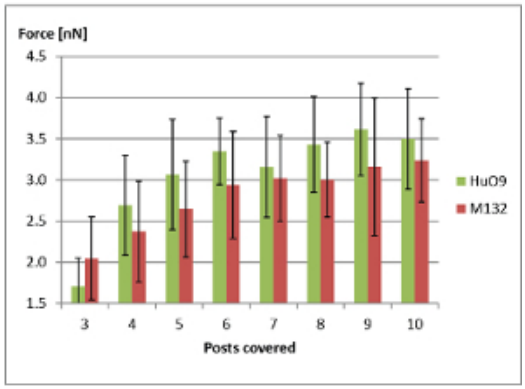

C)

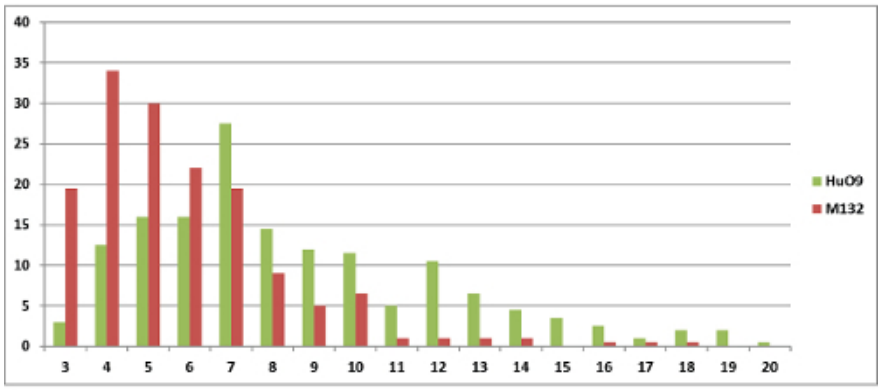

D)

Figure 8. Mechano-profiling of bone cancer cell lines. (**A**) The comparison between the two bone cancer cell lines HuO9 (low metastatic potential) and M132 (highly metastatic) graph shows that all indicator values are higher for the HuO9 cell line (total N=302; two independent sets of experiments, error bar = standard deviation). (**B**) The box plot illustrates that the applied forces per micropost are in the lower nano-Newton range. However, HuO9 cells pull more than M132 cells (Whiskers represent the data minimum and maximum). (**C**) A similar result can be seen by comparing cells that cover the same number of microposts. HuO9 cell apply more force than M132 cells. The number of HuO9 cells covering three microposts is not representative and only included for completeness (error bar = standard deviation). (**D**) The different distributions across the numbers of covered microposts demonstrate that each bone cancer cell line has its own spreading characteristic when interacting with micropost arrays. Please click here to view a larger version of this figure.

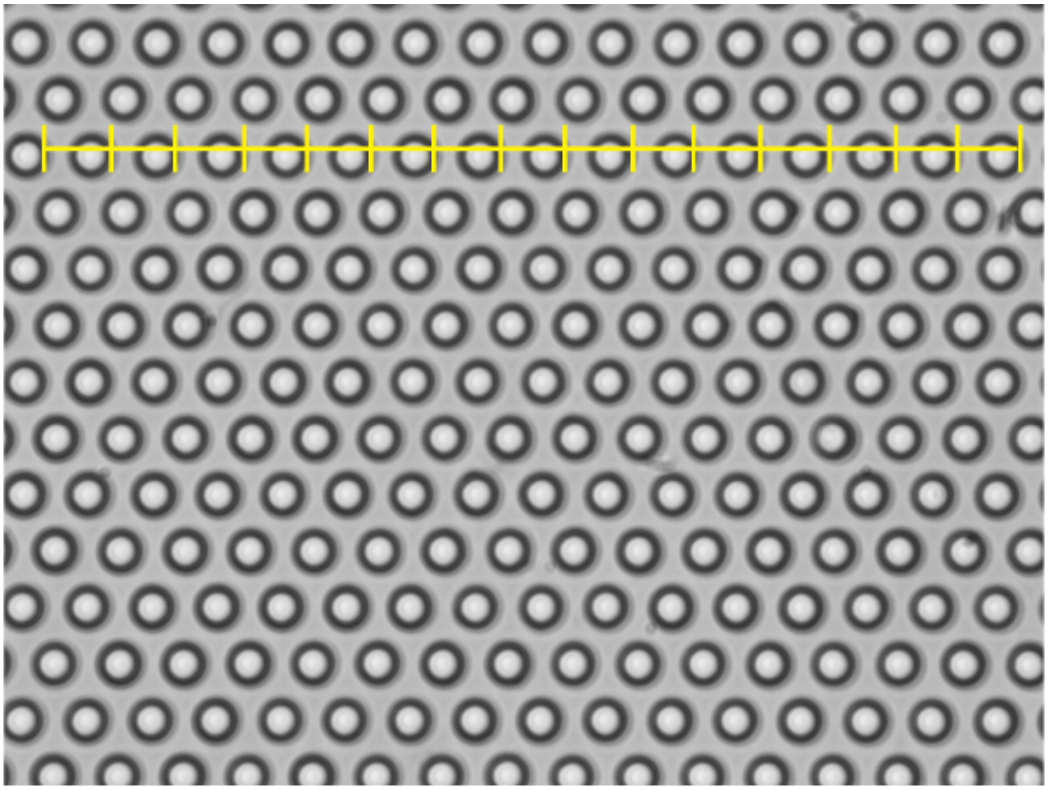

Supplementary Figure 9. The pixel size for a microscope setup is typically determined using a special microscope slide with a scale bar on it; alternatively the micropost array layout, given by the manufacturer can be used. For example, 15 units with 13 microns (195 µm total length) divided by 2,375 pixels (established with an image processing tool) leads to 0.082 µm/pxl. Please click here to view a larger version of this figure.

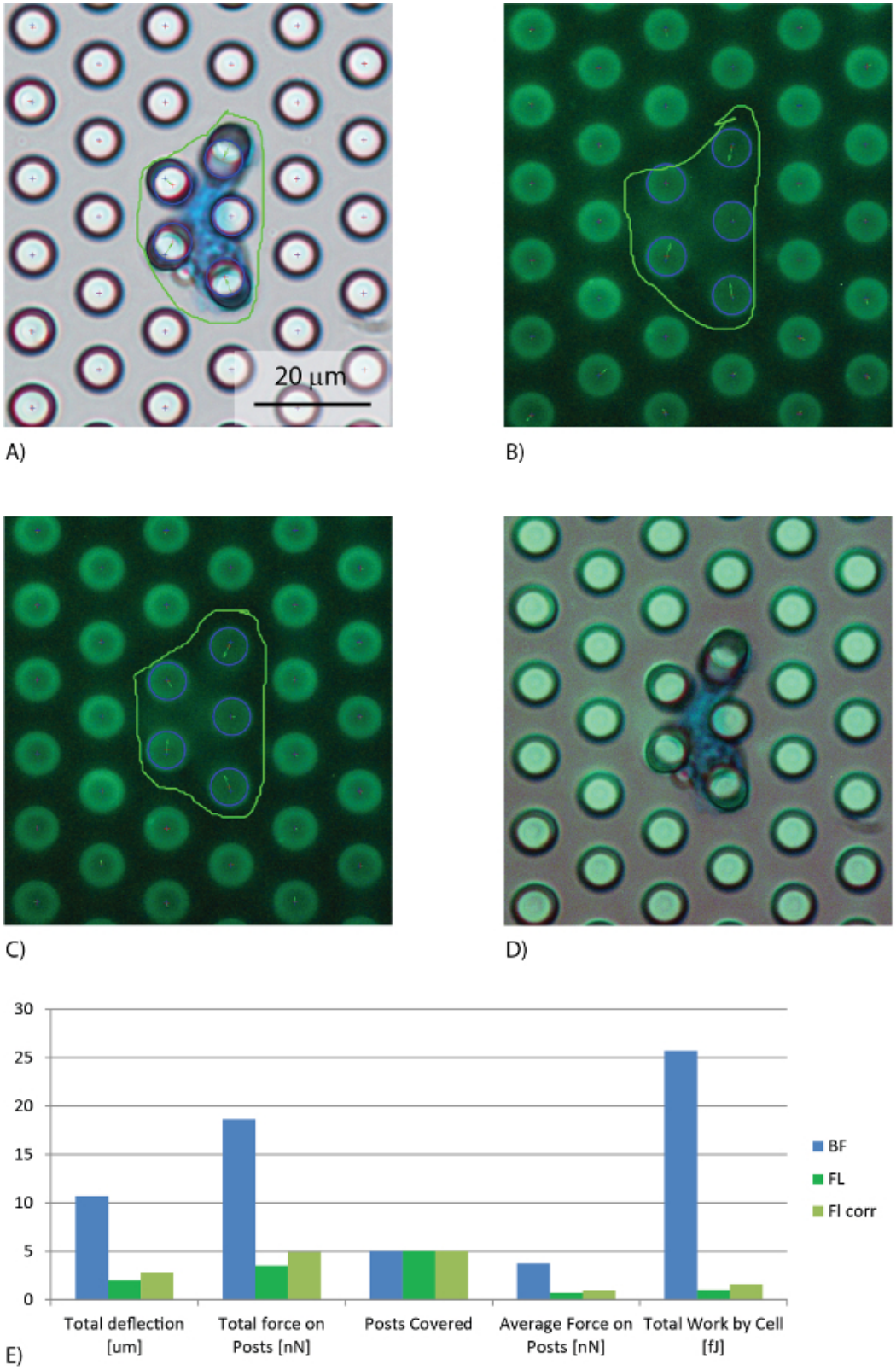

Supplementary Figure 10. Comparison of images of a HuO9 bone cancer cell taken from the same position using two illumination techniques on an inverted microscope; the DiO stained microposts are green fluorescent. (**A**) Analyzed image taken in bright-field mode. (**B**) Analyzed **i**mage taken after switching to the green fluorescence channel without refocusing. (**C**) Second fluorescence image after correcting the focusing to the very micropost tips. (**D**) Overlay of both illumination channels for illustrative purpose only. (**E**) Mechano-profiling indicators as results from the three images. Despite correcting the focus the full deflection cannot be estimated from the fluorescence images. Please click here to view a larger version of this figure.

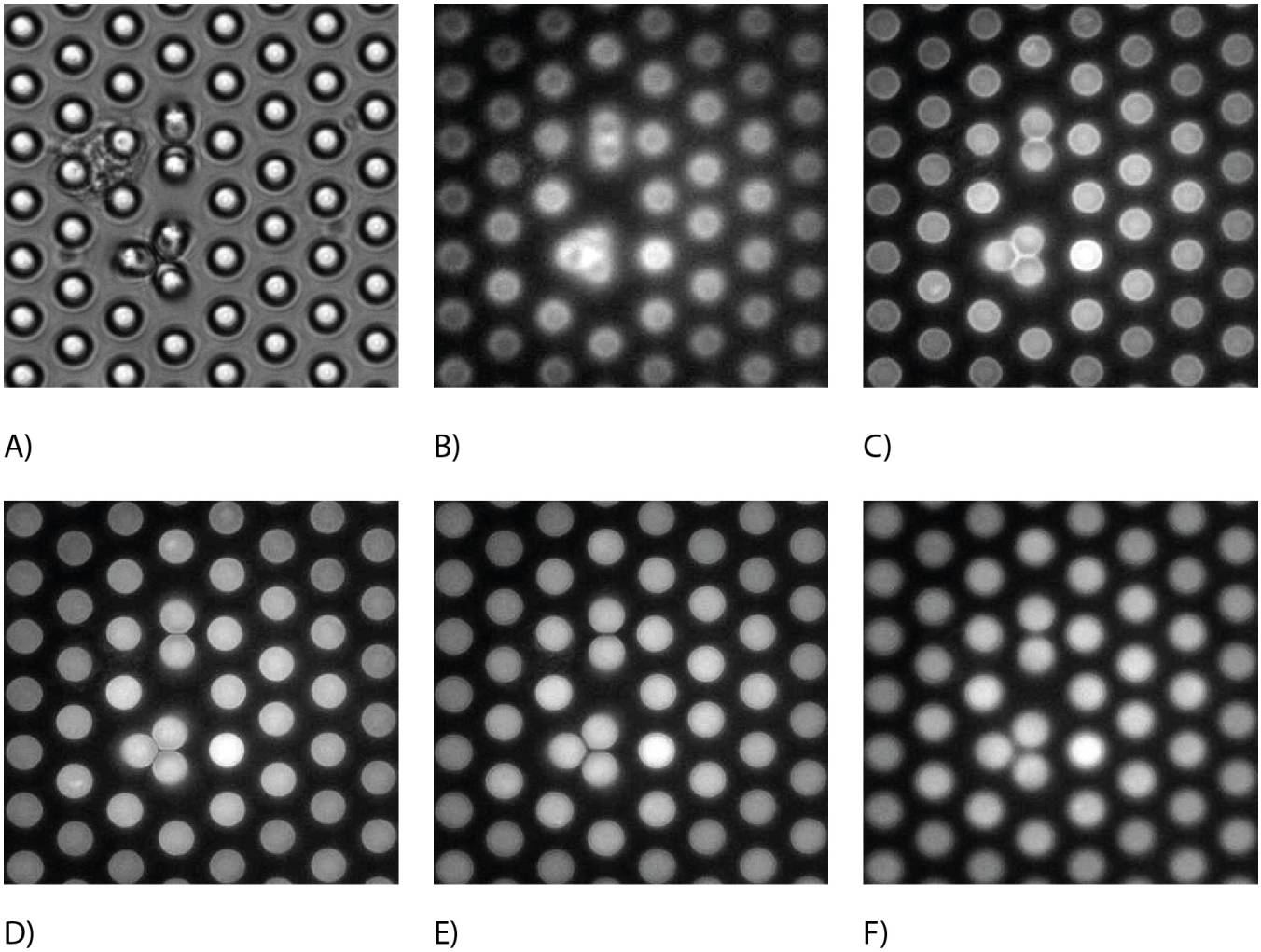

Supplementary Figure 11. Image sequence of the same position of fluorescently stained microposts using DiI on an upright microscope. (**A**) Bright-field image; there are three microposts touching each other at the tip. (**B**) Same position after switching to the fluorescent channel slightly above the microposts' heads. (**C**) Lowering the focal plane to the very tip of the microposts. (**D-E**) Consecutive images after further lowering the focal plane stepwise towards the microposts' bottom. (**F**) Image of the microposts after lowering the focal plane inside the silicone elastomer substrate. Please click here to view a larger version of this figure.

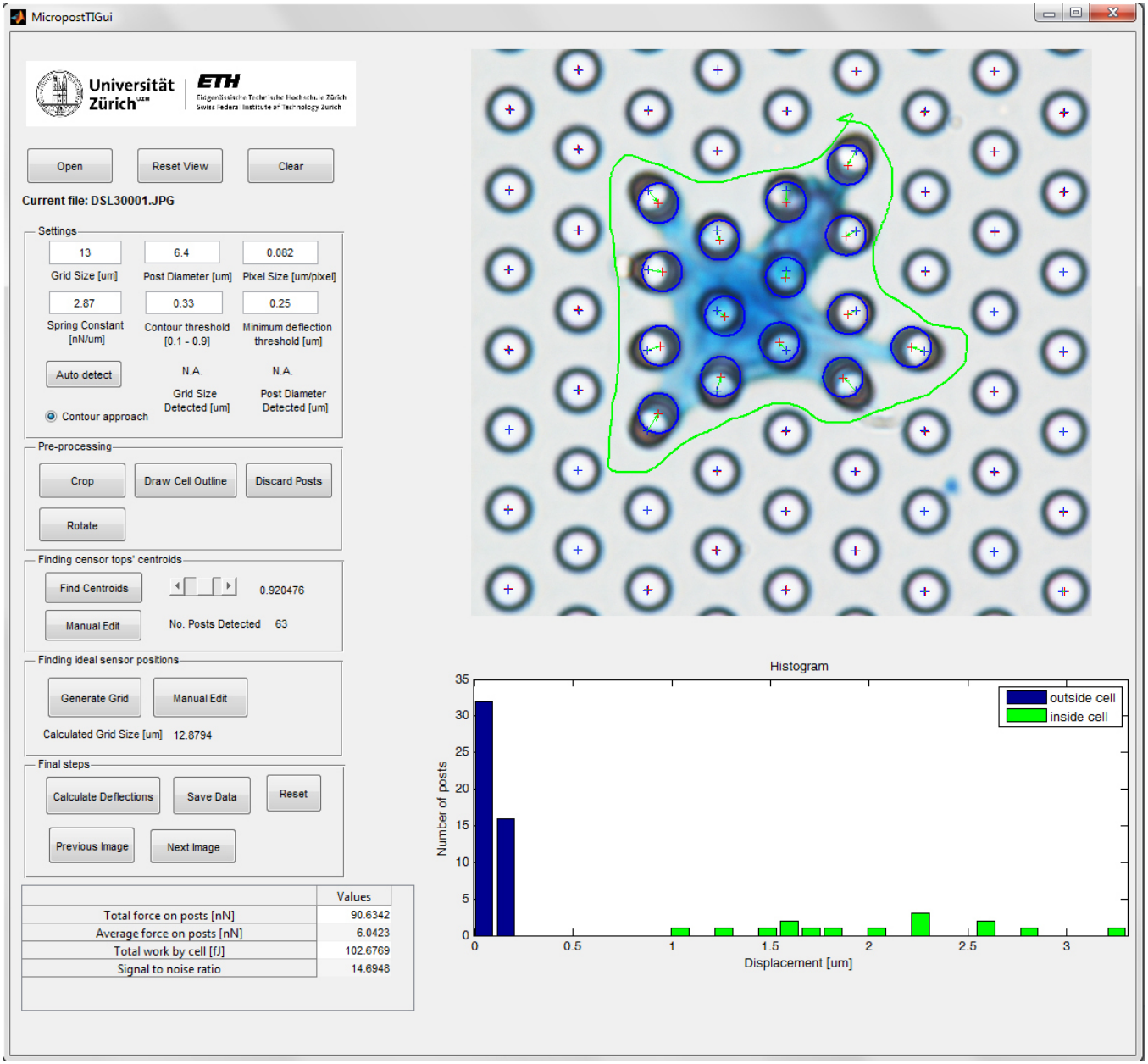

Supplementary Figure 12. Screenshot of the MechProfiler GUI. Typical analysis result from profiling a HuO9 bone cancer cell. Please click here to view a larger version of this figure.

Discussion

This work seeks to advance the field of traction force microscopy by substantially lowering technical and practical barriers to entry. These barriers come from two sides. First and foremost are the numerous non-trivial technical challenges that must be overcome to reproducibly manufacture and experimentally commission a micropost array. Second, is the similarly non-trivial need for a reliable semi-automated analysis of single cell forces – keeping in mind that a typical experiment may require the analysis of hundreds or even thousands of cells. The above described techniques were developed to make micropost based traction force microscopy accessible within cell biology laboratories that do not have resident engineering expertise. The sensors and analysis techniques presented in this article should allow non-experts to readily and accurately analyze the forces exerted by single cells.

Apart from access to a cell biology lab with at least a mid-grade bright-field microscope, the described methods require few additional technical elements. Here most users can perform valid traction force microscopy experiments with even limited experience, despite the power and versatility of the technique. Nonetheless there are three critical aspects in the presented protocol that must be considered. First it is necessary to ensure that the micropost arrays are always covered with liquid to avoid that their collapse due to capillary forces. Second one needs to optimize imaging parameters for acquired micropost images, which is best done by taking series of images of the same array position while varying exposure time, iris aperture, and compensation ring position. It is important to find the correct focal plane for the micropost tip, and this aspect

does take some experience given the small dimensional depth of the sensor arrays. Third one must download the openly accessible image analysis software MechProfiler discussed here, for which a detailed user manual and training examples are available at the download site. After some experience using the software to analyze examples provided with the manual, the user should take test images on the imaging setup to be used so as to configure suitable microscope settings. Based on the obtained images, the contour threshold value should be similarly optimized. A single micropost image can be analyzed by a trained user within a minute using the open-source MechProfiler software regardless of whether it contains one or more cells, allowing the generation of statistically relevant results (analysis of several hundreds of cells) within a few hours.

Another aspect that requires some tuning is the optimization of any applied cell staining procedure. When cells are overly-stained the software can fail to register the correct micropost positions. On the other hand if the staining is too faint it requires more effort by the user to detect a “true” cell outline as thin cell protrusions can be missed.

However, by applying a fixed protocol of cell staining and array imaging procedure the range for this error becomes acceptably low. During this work different cell staining procedures were tested, based on various concentrations of crystal violet, the presence of surfactants like Tween 20 or Triton-X, or a combination of dyes by adding Eosin. Nonetheless, the intensity of the staining as well as its stability varied substantially from experiment to experiment. Only the use of Brilliant Blue G as described above showed an acceptable cell staining robustness combined with enough intensity to still see the thin cell outline but without interfering with the developed contour approach.

In general, there are options to modify the presented technique. For example by combining the bright-field techniques presented here with fluorescence microscopy staining organelles like the nucleus or the actin filament network, which can provide additional information about the underlying cell processes in context of cell mechanics. Furthermore, using long-chain dialkyl carboxycyanines (DiI or DiO) the microposts become fluorescent.[14] Nonetheless, it is important to control each deviation from the presented technique. The supplementary **Figures 10** and **Figure 11** illustrate potential pitfalls. Images taken of a Coomassie Blue G stained NIH 3T3 fibroblast cell in the green fluorescence channel (**Figure 10B and 10C**) using the inverted microscope present the main micropost bodies but not their tips leading to a faulty position analysis (**Figure 10E**). Despite the best effort to refocus after switching from bright-field mode (**Figure 10A**) the micropost tips cannot be imaged, which could be due to absorption of the fluorescence signal by the cell stain. This is in contrast to images taken with the yellow fluorescence channel of an upright microscope (**Figure 11B-11F**) wherein multiple crisp images can be obtain along the z-axis. Here the user needs to ensure that the image is taken with the focal plane at the very tip (**Figure 11C**) and not somewhere closer to the micropost bottom to avoid calling faulty deflection values.

It should be noted that there are also technical limitations for micropost assays. For instance, the accuracy of a detected deflection depends on the quality of the optical setup. Microscopes are often optimized for fluorescence imaging wherein the light sensitivity of the connected camera has a higher priority than a large number of pixels. Naturally, this leads to images with a larger pixel size. Furthermore, it should be noted that bright-field images cannot determine if cell protrusions reach the substrate bottom. However, the commercial micropost arrays were tested using confocal microscopy. It was found that cells seem to accept the binary coating that promotes only adhesion on the micropost tips and not for the rest of the micropost array. Another factor derives from the positional error of the micropost array, which has been shown to be 0.2 µm. Together with the given spring constant of 2.8 nN/µm this leads to an error in force read-out of 0.6 nN. Another constraint for micropost assays derives from the fact that the applied forces from microposts shared by multiple cells cannot be determined. Therefore, only isolated single-cells can be analyzed. A specific limitation for the presented protocol derives from the correct application of the sensitive contour approach, which requires a certain amount of training for the user in order to gain reliable results. Furthermore, for a faster analysis the user should take images wherein the micropost array is aligned to form a horizontal or a vertical line along the edge of the observation field. Despite the fact that the software algorithm for finding microposts within a hexagonal grid geometry is not limited by a rotation angle the imaging of microposts more than 5° off-axis make it difficult to crop to an image section without containing incomplete microposts, which then leads to a failing of the “Generate Grid” function. In such a case the user can use the integrated rotation function before starting to analyze the micropost positions.

The described method was mainly applied to characterize two bone cancer cell lines, a parental cell line named HuO9, and a derived highly metastatic line denominated M132. In this context over six hundred single-cell images were taken in bright field mode and analyzed using the MechProfiler software. The subsequent data mining revealed that the parental cell line HuO9 exerts slightly more force and typically covers more microposts per cell than cells from the metastatic cell line M132. However the cells were not synchronized and therefore in different stages of cell cycle at the moment of fixation, which likely contributed to the broad range of results. By taking live cell images over time periods of up to 24 hr, it was found that after spreading many cells remain at their initial position whereas others migrate, spread, disconnect and migrate again with different velocities (see supplementary videos). This indicates that the mechanical profile of a cell is often not constant and can vary greatly across a cell population or even within a single cell depending on its current activity. Another contributing factor could be that on a micropost array a cell is forced to perform discrete migration steps to reach another micropost, which is in contrast to classic TFM, where cells adhere to flat surfaces and can migrate with minute steps. However, in order to analyze these small steps it is necessary to take fluorescent images of focal adhesion points, which requires access to very advanced microscopes and highly elaborate image analysis software. Nonetheless, the distribution of mechanical profiles within larger populations is still often a defining characteristic of a cell line. Thus a high-throughput method that enables characterization of a large number of cells is essential. The manual imaging process and open-access software presented here harbors great potential for scaling to fully automatic microscope systems.

In summary a robust traction force microscopy approach is presented that is readily adoptable in a standard cell biology lab. The entire workflow from cell seeding to image analysis is simple and effective. While the protocols described here are fully functional, improvements are ongoing to adapt the analysis algorithms to be able to also handle micropost arrays with orthogonal layouts and developing procedures that simplify the analysis of image sequences from live cell imaging. In context with the results for bone cancer cell lines, the approaches described here can be used to screen cells from clinical biopsies in order to establish whether such assays may hold prognostic value, enabling clinicians to predict the metastatic potential of biopsied cells from bone cancer patients. Such an assay would influence the therapeutic strategies. Other potential applications relate to testing pharmaceutically active compounds on mechanically active cells like smooth muscle cells or cardiomyocytes, potentially to assist in establishing a drug’s efficacy or toxicity.

Disclosures

The lead author (NG) is co-founder of MicroDuits GmbH, the commercial supplier of the micropost arrays used in this study. No other authors have any potential conflicts of interest with this work.

Acknowledgements

This work was supported by the Committee Technology and Innovation (CTI) Switzerland grant 14796-PFLS-LSCTI. MicroPost arrays were generously provided by MicroDuits GmbH.

References

1. Sharma, R.I., & Snedeker, J.G. Biochemical and biomechanical gradients for directed bone marrow stromal cell differentiation toward tendon and bone. *Biomaterials.* **31** (30), 7695-7704, (2010).
2. Suresh, S. Biomechanics and biophysics of cancer cells. *Acta Biomater.* **3** (4), 413-438, (2007).
3. Bartalena, G. *et al.* A novel method for assessing adherent single-cell stiffness in tension: design and testing of a substrate-based live cell functional imaging device. *Biomed Microdevices.* **13** (2), 291-301, (2011).
4. Tan, J.L. *et al.* Cells lying on a bed of microneedles: An approach to isolate mechanical force. *PNAS.* **100** (4), 1484-1489, (2003).
5. Akiyama, Y., Hoshino, T., Iwabuchi, K., & Morishima, K. Room Temperature Operable Autonomously Moving Bio-Microrobot Powered by Insect Dorsal Vessel Tissue. *PloS ONE.* **7** (7), (2012).
6. Biais, N., Ladoux, B., Higashi, D., So, M., & Sheetz, M. Cooperative retraction of bundled type IV pili enables nanonewton force generation. *Plos Biology.* **6** (4), 907-913, (2008).
7. Wuang, S.C., Ladoux, B., & Lim, C.T. Probing the Chemo-Mechanical Effects of an Anti-Cancer Drug Emodin on Breast Cancer Cells. *Cell Mol Bioeng.* **4** (3), 466-475, (2011).
8. Schoen, I., Hu, W., Klotzsch, E., & Vogel, V. Probing Cellular Traction Forces by Micropillar Arrays: Contribution of Substrate Warping to Pillar Deflection. *Nano Lett.* **10** (5), 1823-1830, (2010).
9. Lemmon, C.A. *et al.* Shear Force at the Cell-Matrix Interface: Enhanced Analysis for Microfabricated Post Array Detectors. *Mech Chem Biosyst.* **2** (1), 1-16, (2005).
10. Lam, R.H.W., Weng, S.N., Lu, W., & Fu, J.P. Live-cell subcellular measurement of cell stiffness using a microengineered stretchable micropost array membrane. *Integr Biol-UK.* **4** (10), 1289-1298, (2012).
11. Roure, O. *et al.* Force mapping in epithelial cell migration. *PNAS.* **102** (39), 14122-14122, (2005).
12. Papenburg, B.J., Rodrigues, E.D., Wessling, M., & Stamatialis, D. Insights into the role of material surface topography and wettability on cell-material interactions. *Soft Matter.* **6** (18), 4377-4388, (2010).
13. Badique, F. *et al.* Directing nuclear deformation on micropillared surfaces by substrate geometry and cytoskeleton organization. *Biomaterials.* **34** (12), 2991-3001, (2013).
14. Sniadecki, N.J. *et al.* Magnetic microposts as an approach to apply forces to living cells. *PNAS.* **104** (37), 14553-14558, (2007).
15. Mann , J.M., Lam , R.H.W., Weng , S., Yubing, S., & Fu, J. A silicone-based stretchable micropost array membrane for monitoring live-cell subcellular cytoskeletal response. *Lab Chip.* **12**, 731-740, (2012).
16. Desai, R.A., Yang, M.T., Sniadecki, N.J., Legant, W.R., & Chen, C.S. Microfabricated Post-Array-Detectors (mPADs): an Approach to Isolate Mechanical Forces. *J Vis Exp.* (8), e311, (2007).
17. Yang, M.T., Fu, J.P., Wang, Y.K., Desai, R.A., & Chen, C.S. Assaying stem cell mechanobiology on microfabricated elastomeric substrates with geometrically modulated rigidity. *Nat Protoc.* **6** (2), 187-213, (2011).
18. Sniadecki, N. J., Han, S. J., Ting, L. H., & Feghhi, S. in Micropatterning in Cell Biology *Methods in Cell Biol.* **121** (5) 61-73,doi: 10.1016/B978-0-12-800281-0.00005-1 (2014).

